applied sciences

MDPI

Article

Detrital Mica Composition Quantitatively Indicates the Sediment Provenance along the Subei Coast to the Yangtze Estuary

Zhicheng Dong [1,2], Lina Zhang [1,2,*] and Bingfu Jin [3,*]

[1] School of Geographic Sciences and Tourism, Jiaying University, Meizhou 514015, China
[2] Guangdong Provincial Key Laboratory of Conservation and Precision Utilization of Characteristic Agricultural Resources in Mountainous Areas, Jiaying University, Meizhou 514015, China
[3] School of Resources and Environmental Engineering, Ludong University, Yantai 264025, China
* Correspondence: zhanglina_2005@126.com (L.Z.); bingfu_jin@163.com (B.J.)

Abstract: The influence of large rivers on the Subei littoral plain area requires more research than the results that have been available up to now. Thus, specific diagnostic indices of detrital mica are successfully applied for the first time to identify the detritus of the Yangtze River and the ancient Yellow River and to analyze their influence on the coast in the Subei littoral plain area. Based on field investigation and sample collection, detrital mica minerals within the 0.063–0.125 mm grain size fraction were selected and identified. Their content/ratio differentiations and possible origins were analyzed. Moreover, specific diagnostic indices were evaluated for detritus identification considering these two large rivers in addition to their provenance influences on the Subei littoral plain area. The results indicate that the detrital mica contents in the Yangtze River Estuary differed from those in the ancient Yellow River Estuary. The mass percentage in the former (average value of 32.2%) was much higher than that in the latter (average value of 13.1%). The former contained abundant weathered mica, with a particle percentage of approximately 50.6%, while the latter contained abundant biotite (with a particle percentage of approximately 40.9%). Differences, including but not limited to those above, could be attributed to basic geological, climatic and hydrodynamic conditions. In particular, the mica indices were clearly distinguished between these two river estuaries. These indices constitute specific diagnostic indices for differentiating river detritus and quantitative contribution analysis of detritus provenance in the Subei littoral plain area. Finally, the changes and quantitative contributions of four diagnostic indices demonstrated that in the Subei littoral plain area, northward from the Yangtze River Estuary to sample site SBY11 located in Yangkou town, Rudong County, detrital micas were mainly affected by the Yangtze River, and southward from the ancient Yellow River Estuary to sample site SBY12 located in Bengcha town, Rudong County, detrital micas were largely affected by the ancient Yellow River. The main mixing area should be located between these two towns. This study provides both a good example and an efficient approach to the application of detrital mica in detritus identification, mixed zone determination, sediment provenance analysis and transport tracing.

Keywords: mica; muscovite; biotite; muscovite; weathered mica; provenance analysis; Yangtze River; ancient Yellow River; Subei littoral plain area

Citation: Dong, Z.; Zhang, L.; Jin, B. Detrital Mica Composition Quantitatively Indicates the Sediment Provenance along the Subei Coast to the Yangtze Estuary. *Appl. Sci.* **2022**, *12*, 12653. https://doi.org/10.3390/app122412653

Academic Editor: Eduardo Ferreira da Silva

Received: 10 November 2022
Accepted: 7 December 2022
Published: 9 December 2022

1. Introduction

The Yangtze River and Yellow River play significant roles in the formation and evolution of the eastern coastal zone and continental shelf of China [1]. The identification of their river sediments represents a basic problem in provenance research [2]. The Subei littoral plain area is representative of the East China continental shelf. Sediment mixing and diffusion of the Yangtze River and Yellow River, especially their material contributions, still remain to be further studied and explained [3]. Thus, based on theories of genetic mineralogy and marine geology, numerous studies on sediment identification in these two large rivers, as well as provenance tracing across the Subei littoral plain area have been performed by evaluating the provenance significance of typomorphic minerals and their assemblage, as well as the typomorphic characteristics of minerals, and these studies have yielded numerous and substantial achievements [1,2,4–6]. For instance, the results demonstrated that differences between the sediments in these two large rivers could be found in terms of clay mineral contents [6–8], ratios [9], crystallinity [7,9], chemical indices [9], crystal shapes [10], geochemical characteristics [10], etc., including indicators of detritus identification [7,8]. Previous results also revealed differences in carbonate mineral contents [11–14], crystal shapes [12], grain size effects [12], abrasion and dissolution characteristics [15], etc., which could be used as tracing indices of the Yangtze River and Yellow River [11] to indicate the provenance of sediments on the continental shelf [12]. Other studies have suggested that indicators such as the crystal shape [16], light and/or heavy mineral assemblages [4,11,17,18], geochemical composition [5,6,19,20], magnetite content and other magnetic parameters [2,21,22] could also be applied to distinguish these two large rivers and the sediment provenance [4,5,17,23] of the Yellow Sea and East Sea. In addition, previous results indicated that Yellow River sediments were characterized by high mica mineral contents [24,25]. This finding could be considered for source identification, material diffusion, coastline changes and paleogeographic environment evolution [25]. Moreover, research has revealed that the heavy mineral assemblage of fine-grained (0.063–0.125 mm) sediments was basically characterized by a high content of schistose mica minerals (up to 60%) in the Yangtze River Estuary [26]. Compared with granular minerals, such as quartz and feldspar, schistose mica minerals, they exhibit different behaviors during migration and deposition [27–29]. Moreover, results show that mica $^{40}Ar/^{39}Ar$-dating has important implications for future provenance studies [30,31]. Thus, mica could theoretically be employed as an indicator for sediment transport and diffusion [32]. The mica content difference could be applied to distinguish between Yangtze River and Yellow River provenances [33]. However, relevant research on this topic is largely lacking. Certain questions still require further study. For example, what are the specific differences in detrital mica minerals in sediments between the Yangtze River and Yellow River? Could these differences be employed as specific diagnostic indices? Could these indices be applied to analyze detritus mixing and diffusion along the coast of the Subei littoral plain area?

Based on the above information, this study compares the differences in the contents and ratios of detrital mica in sediments between the Yangtze River Estuary and the ancient Yellow River Estuary. The possible causes of these differences were also analyzed. Consequently, reliable specific diagnostic indices of detrital mica were examined and distinguished for detritus identification between these two rivers. Then, the mixed area of detrital mica along the coast of the Subei littoral plain area was analyzed. In addition, the ranges of influence of these two large rivers were preliminarily evaluated. This study could provide both a good example and an efficient approach to the application of detrital mica in detritus identification, mixed zone determination, sediment provenance analysis and transport tracing. These efforts could help to provide new ideas and references to examine and distinguish specific diagnostic indices of sediment sources, as well as for provenance analysis in the Subei littoral plain area and even the East China continental shelf.

This work is organized as follows. In Section 2, the regional settings are reviewed and the research materials and methods, such as field investigation and surface sediment sample collection, mineral separation and identification are also described. In Section 3, the experiment results are described and analyzed. In Section 4, the implications and extensions of the results of Section 3 are discussed. Finally, Section 5 presents research conclusions.

2. Regional Settings and Methods

2.1. Regional Settings

(1) Yangtze River (Changjiang)

As shown in Figure 1, The Yangtze River (24°–35° N, 90°–122° E) is the largest river in China, with a length of approximately 6300 km and a drainage area of 1.81 × 10^6 km^2 [34]. The entire drainage area is controlled by temperate and subtropical climate types, with an annual average precipitation of approximately 1100 mm. The geological background in the drainage area is complex. The Yangtze River spans the South China Orogenic Belt, Yangtze Platform, Qinling-Dabie Orogenic Belt, Sanjiang Paleotethys and other tectonic units. The lithology in the drainage area is varied, comprising clastic sedimentary, metamorphic and igneous rocks. Research has demonstrated that the annual average sediment discharge reaches 0.5 × 10^9 t due to the high sediment content upstream and north of the drainage area [34]. Approximately 50% of the sediments are deposited near the estuary [34]. In addition, seaward sediments originating from the Yangtze River are mainly towards the southeast, with a smaller northward component. Sediment is exchanged with the coast of the Subei littoral plain area.

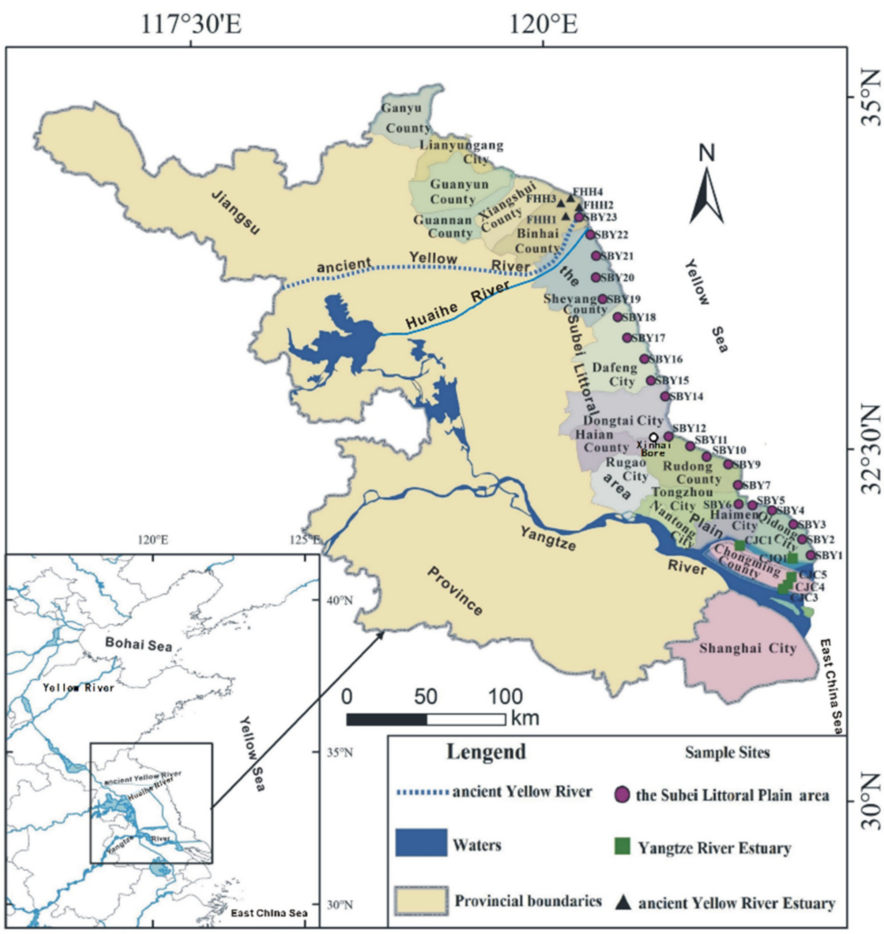

Figure 1. Study area and sampling sites. GPS point information can be found in Appendix A.

(2) Ancient Yellow River

The ancient Yellow River (Figure 1), also referred to as the waste Yellow River, is located in the northern Huaihe River drainage area. This river is an old course of the Yellow River and flows from the north of Lankao city in Henan Province toward the southeast, passing through Minquan County, north of Shangqiu city in Dangshan County in Anhui Province, north of Xuzhou city in Jiangsu Province, south of Suqian city and north of

Huai'an city; then, the river turns northeast, flowing to the south of Lianshui County and north of Binhai County, and entering the Yellow Sea at Taowan village, where the ancient Yellow River Estuary is located. Its downstream channel is also the sea channel of the ancient Huaihe River. According to historical records, the Yellow River has changed its course 11 times throughout history. During the Pleistocene and more recent historical periods, the Yellow River entered the sea in northern Jiangsu many times [35,36]. Research has indicated that the Yellow River' annual average sediment discharge in the estuary reaches 8.39×10^8 t [37] since the main provenance area is widely covered with loess [38]. Thus, the Yellow River is well known worldwide for its high concentration of fine clay and sand. As the Yellow River migrated and captured the Huaihe River, a large amount of sediments was entrained and transported. Fine-grained detritus was rapidly dominated by silty clay deposits. This change caused the land and underwater deltas of the ancient Yellow River to rapidly prograde. In particular, the coastline rapidly prograded. After 1855, the Yellow River merged into the Bohai Sea in the north. Research has revealed that approximately 90% of the detritus entering the sea by way of the Yellow River originates from the Loess Plateau in the midstream region, which is the main source of surface sediments along the northern Jiangsu coast [39].

(3) Subei littoral plain area

The Subei littoral plain area is located between the Yangtze River Delta and ancient Yellow River Delta (Figure 1). It is a wide plain formed by the development and accumulation of ancient bays under the interaction of rivers and the sea during the Quaternary Period [40]. It is generally accepted that the Subei littoral plain area was formed under the combined action of tides and seagoing rivers, such as the Yangtze River and the ancient Yellow River [40]. As the main controlling factors, the detritus carried by these two rivers are the main material sources of the Subei littoral plain area. However, before the last capture of the Huaihe River by the ancient Yellow River entering the sea, the main detritus source of the Subei littoral plain area included northward components of Yangtze River sediments. Since the amount of northward components was small, coastlines remained relatively stable for a long time. Nevertheless, the ancient Yellow River captured the Huaihe River and entered the sea in 1128. This provided a large amount of detritus for the formation of the Subei littoral plain area. A previous study demonstrated that the northern Jiangsu coast was mainly affected by the Yellow River [41]. Major element content changes suggested that northward diffusion of Yangtze River sediments was weak and ranged from the estuary to Rudong County [42]. Montmorillonite content changes indicated that the coast northward from Rudong County to the ancient Yellow River Estuary comprised ancient Yellow River detritus [42]. Yang et al. proposed that the land formation process in the Subei littoral plain area was mainly controlled by Yellow River detritus, which could affect areas as far south as the area near Xinhai Bore [43]. Li et al. suggested that sediments from the coast southward from Rudong County to the Yangtze River Estuary were dominated by Yangtze River sediments, while sediments from the coast northward from Dafeng County to the ancient Yellow River Estuary were dominated by Yellow River sediments [44]. The sediments between these two counties were mixtures of the sediments of these two large rivers [44]. Based on clay mineral assemblages, Yi et al. proposed that sediments from the coast northward from Rudong County to the ancient Yellow River Estuary were dominated by Yellow River inputs, whereas those from the coast southward from Rudong County to the Yangtze River Estuary were dominated by Yangtze River inputs [45]. As mentioned above, in the Subei littoral plain area, the ranges of influence and mixed areas of these two large rivers remain controversial.

(4) Currents Tides and Sediment Transportation

Fruitful research on tidal currents and sediment transport along the Subei coast has been performed in recent decades. The vast majority of the obtained results have indicated that under the influences of the Yellow sea coastal current (YSCC) and Subei coastal waters (SCWs) in winter, suspended sediments around the ancient Yellow River Estuary are transported to the southeast toward the radial sand ridge, even to areas near the Yangtze River Estuary, and jointly with Yangtze River sediments they are carried toward Jeju Island [46]. However, other studies have demonstrated that there is a northward flow along the Subei coast [47], and this could probably cause sediment flow from the ancient Yellow River Estuary or even from the radial sand ridge and the Yangtze River Estuary northward to Haizhou Bay [48]. Zhao et al. also proposed that the tidal residual current flowing northward along the coast could transport sediments into SCWs [49]. Xia et al. [50] also found that there exists a relatively stable northward low-frequency circulation along the Subei coast in summer, which flows northward from the north branch of the Yangtze Estuary to Haizhou Bay, turns east and then flows southeast, and this circulation could probably transport Yangtze River sediments to replenish the Subei coast. Wu et al. also determined that the direction of the coastal current in Subei is upwind in winter, and this could probably provide new ideas to explain the source-sink relationship between the Yangtze River Estuary and Subei littoral plain area, combined with the fate of materials entering the sea from the Yangtze River [51]. In summary, it could be concluded that sediment transportation along the Subei coast and the material contributions of the ancient Yellow River and Yangtze River to the Subei littoral plain area are complex and should be investigated.

2.2. Methods

2.2.1. Sampling

Sediment samples were collected via shovel sampling and were hermetically sealed in polythene bags. A total of 30 surface sediment samples were collected in March 2016. In detail, as shown in Figure 1, five sediment samples in the Yangtze River Estuary (CJC1, CJC3, CJC4, CJC5, and CJQ1), twenty-one sediment samples in the Subei littoral plain area (SBY1-SBY7, SBY9-SBY12, and SBY13-SBY23), and four sediment samples in the ancient Yellow River Estuary (FHH1, FHH2, FHH3, and FHH4) were collected from subsurface floodplains along the coast at a depth ranging from 0–10 cm. Sample sites far away from pollution sources are shown in Figure 1.

2.2.2. Mineral Separation and Identification

Mineral separation and identification conducted as follows. Approximately 100–200 g of each sediment sample were wet sieved to obtain the very fine sand fraction (0.063–0.125 mm) via nylon mesh screens. Additionally, the very fine sand fraction of each subsample was dried and weighed. Then, each subsample was placed into bromoform (CHBr3, ρ = 2.65–3.15 g/cm^3) and centrifugalized to separate the detrital micas. This was repeated until almost no mica could be separated. Then, the obtained micas were manually purified by removing other minerals under the microscope. Additionally, micas left in the very fine sand fraction subsample were manually selected under the microscope. After repeatedly rinsing with alcohol, all the obtained detrital micas were dried at 60 °C and weighed to calculate the mass percentage. Finally, the Gazzi-Dickinson method [52] was used for the mica identification under the microscope. In detail, line counts of 300–500 grains were identified under a binocular microscope with incident light. Particles of biotite, weathered mica, and muscovite were classified (Figure 2) and counted.

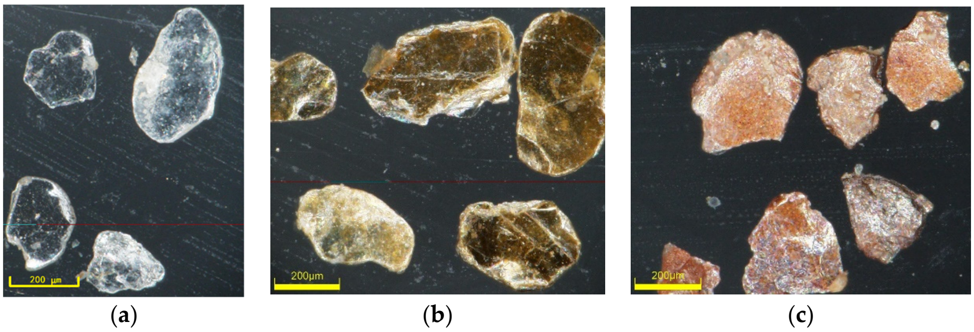

Figure 2. Muscovite (**a**), biotite (**b**) and weathered mica (**c**) under the microscope.

The particle percentages of biotite, weathered mica, and muscovite were separately calculated as follows: particle percentage of biotite or weathered mica or muscovite = 100% * particle number of biotite or weathered mica or muscovite/total particle number of mica. Additionally, the mass percentage of mica was calculated as follows: mass percentage of mica = 100% * total mica mass/total mineral mass.

2.2.3. Multivariate Statistical Analysis and Calculation of Provenance Contribution

Multivariate statistical analysis and the charts were conducted by using the Statistica Software v.6.0 (Palo Alto, CA, USA).

Based on quality conservation, countless sediment provenances and the mathematical model of nonlinear programming [53], we believe that detrital micas in the very fine sand fraction of sediments in the Yangtze River, the ancient Yellow River, and other unknown sources, all contribute to the Subei littoral plain area. Additionally, there is a certain linear mathematical relationship between them. This relationship can be calculated by the following mathematical model:

$$Y_i = a_1 Y_{1i} + a_2 Y_{2i} + \varepsilon_i \quad (1)$$

where Y_i is the value of mica-specific diagnostic index *i* in the very fine sand fraction of the Subei littoral plain area sediments, Y_{1i} is the value of mica-specific diagnostic index *i* in the very fine sand fraction of the Yangtze River sediments, Y_{2i} is the value of mica-specific diagnostic index *i* in the very fine sand fraction of the ancient Yellow River sediments, ε_i is the contribution of mica-specific diagnostic index *i* in other unknown sources, a_1 is the contribution percentage of the Yangtze River, a_2 is the contribution percentage of the ancient Yellow River, i is the serial number of the mica-specific diagnostic index (i = 1, . . . , n).

3. Results

3.1. Mica Contents in the Very Fine Sand Fraction of Yangtze Estuary Sediments

The mass percentage of mica, the particle percentages of biotite, weathered mica and muscovite significantly differed among the samples of the very fine sand fraction collected in the Yangtze River Estuary (Figure 3). Specifically, the mass percentage of mica was high, with an average value of 32.2% and a maximum content of 57.3%. The particle percentage of weathered mica was the highest, with a value of approximately 50.6%, and the highest content reached 65.7%, followed by muscovite, with an average particle percentage of 37.2%. The particle percentage of biotite was the lowest, with a value of only approximately 12.3%, and the highest content reached only 19.8%.

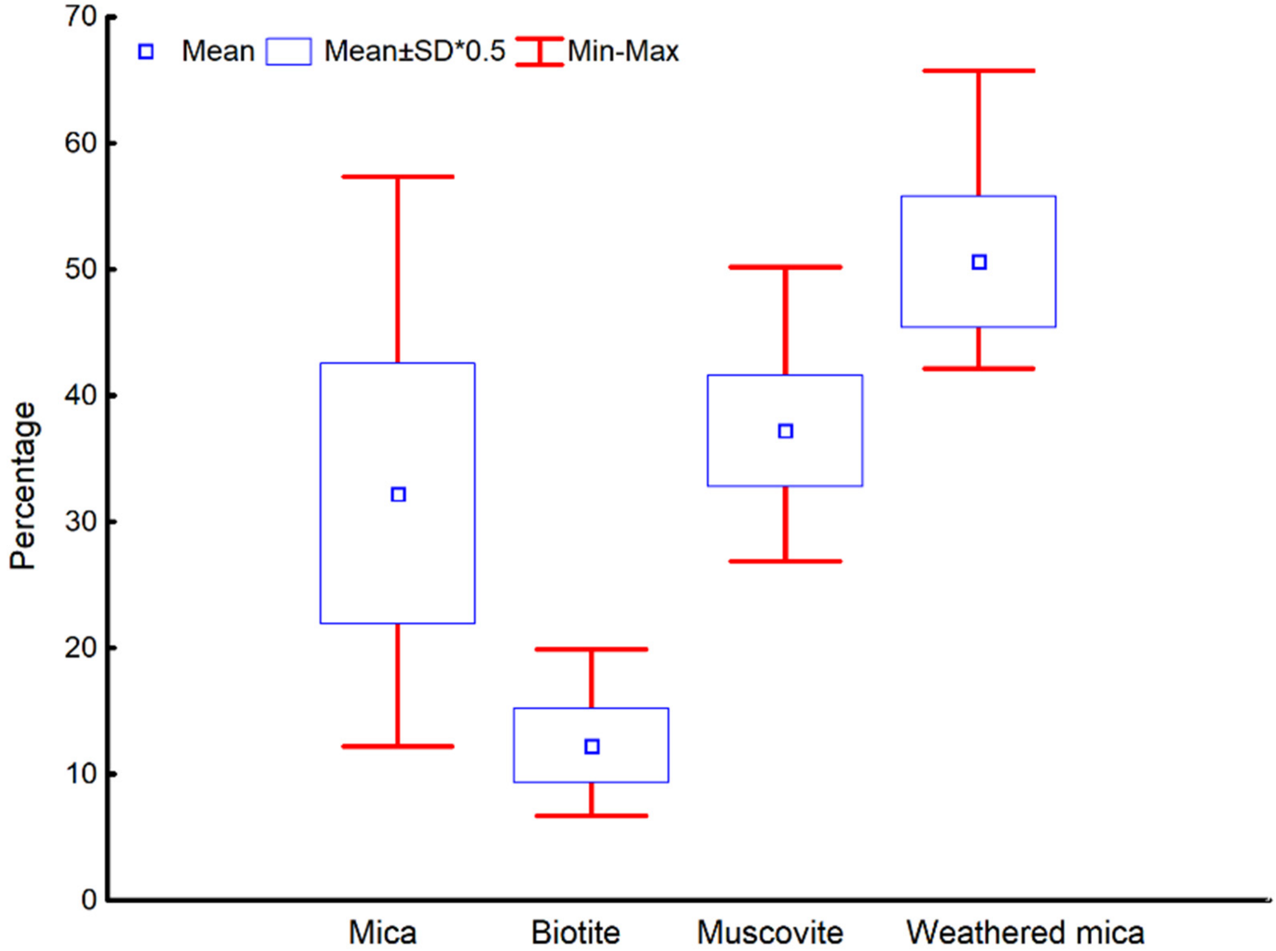

Figure 3. Mass percentage of mica, particle percentages of biotite, weathered mica and muscovite in the very fine sand fraction of the collected Yangtze River Estuary sediment samples (mass percentage of mica = 100 * total mica mass/total mineral mass. Particle percentage of biotite or weathered mica or muscovite = 100 * particle number of biotite or weathered mica or muscovite/total particle number of mica).

3.2. Mica Contents in the Very Fine Sand Fraction of Ancient Yellow Estuary Sediments

The mass percentage of mica and the particle percentages of biotite, weathered mica and muscovite obviously varied among the samples of the very fine sand fraction collected in the ancient Yellow River Estuary (Figure 4). In detail, the mass percentage of mica was low, with a mean value of only 13.1%. The mass percentages in most samples were low, ranging from 1% to 5%, except for sample FHH3, which exhibited a higher value of 47.5%. Comparison and analysis of the particle percentage differences among biotite, muscovite and weathered mica revealed that biotite was the main mica type in the very fine sand fraction of the sediment samples, with a particle percentage of 40.9%, followed by muscovite, with an average particle percentage of 32.3%, slightly lower than that of biotite. The particle percentage of weathered mica was the lowest, with a value of only approximately 26.8%.

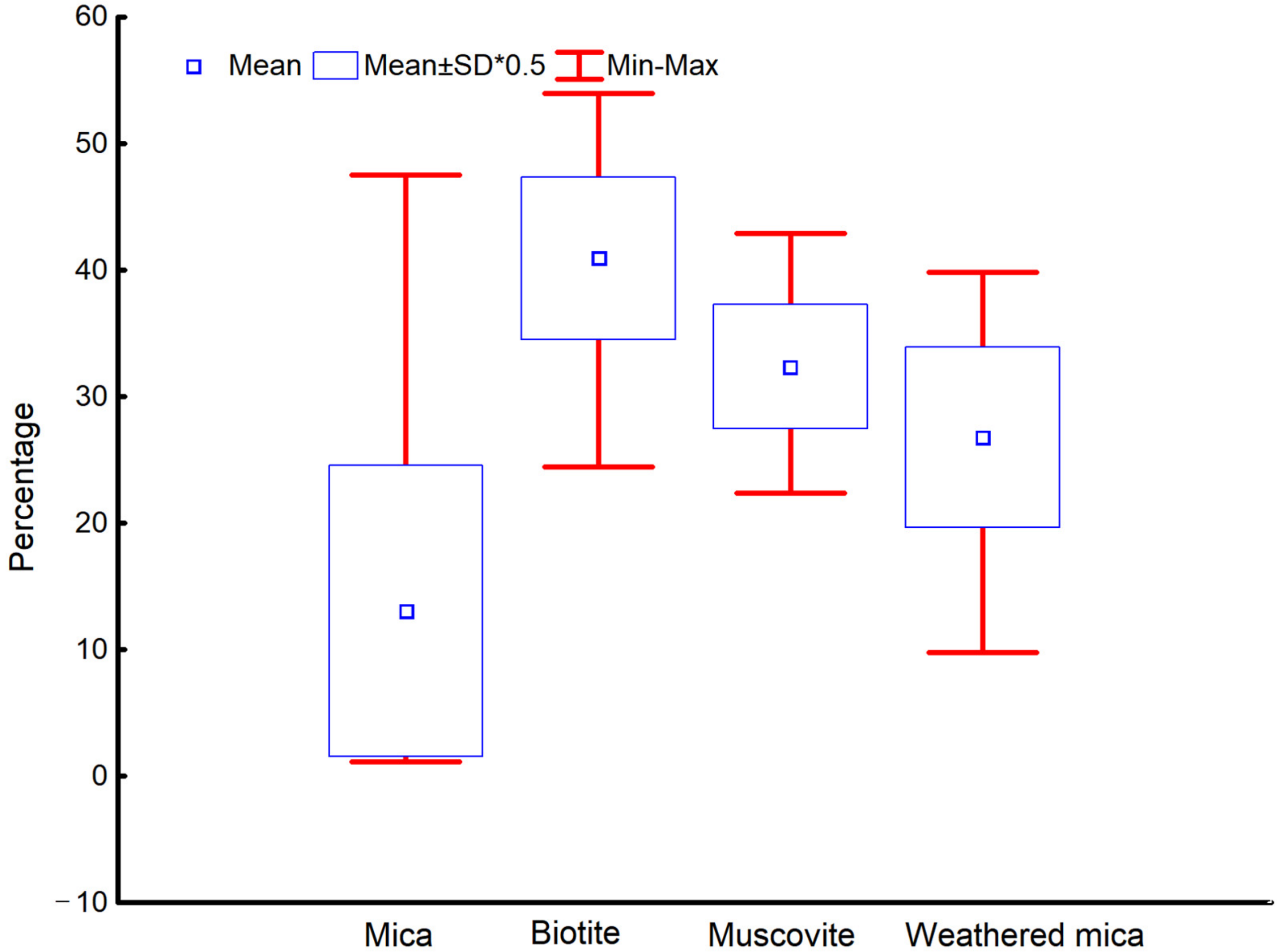

Figure 4. Mass percentage of mica, particle percentages of biotite, weathered mica and muscovite in the very fine sand fraction of ancient Yellow River Estuary sediments (mass percentage of mica = 100 * total mica mass/total mineral mass. Particle percentage of biotite or weathered mica or muscovite = 100 * particle number of biotite or weathered mica or muscovite/total particle number of mica).

3.3. Mica Contents in the Very Fine Sand Fraction of Subei Littoral Plain Area Sediments

The mass percentage of mica, the particle percentages of biotite, weathered mica and muscovite obviously differed among the various samples of the very fine sand fraction of coastal sediments of the Subei littoral plain area (Figure 5). More specifically, the mass percentage of mica was very high, with an average value of up to 43.3%. The dispersion of the mass percentage data was very high, with the standard deviation reaching 24.3. By comparing and analyzing the particle percentage differences among biotite, muscovite and weathered mica, the results indicated that muscovite was the main mica type in the very fine sand fraction of the sediment samples collected in the Subei littoral plain area, with an average particle percentage of 40.9%. The average particle percentage of weathered mica was 33.0%, which is slightly lower than that of biotite. The particle percentage of biotite was the lowest, with a value of only approximately 26.2%.

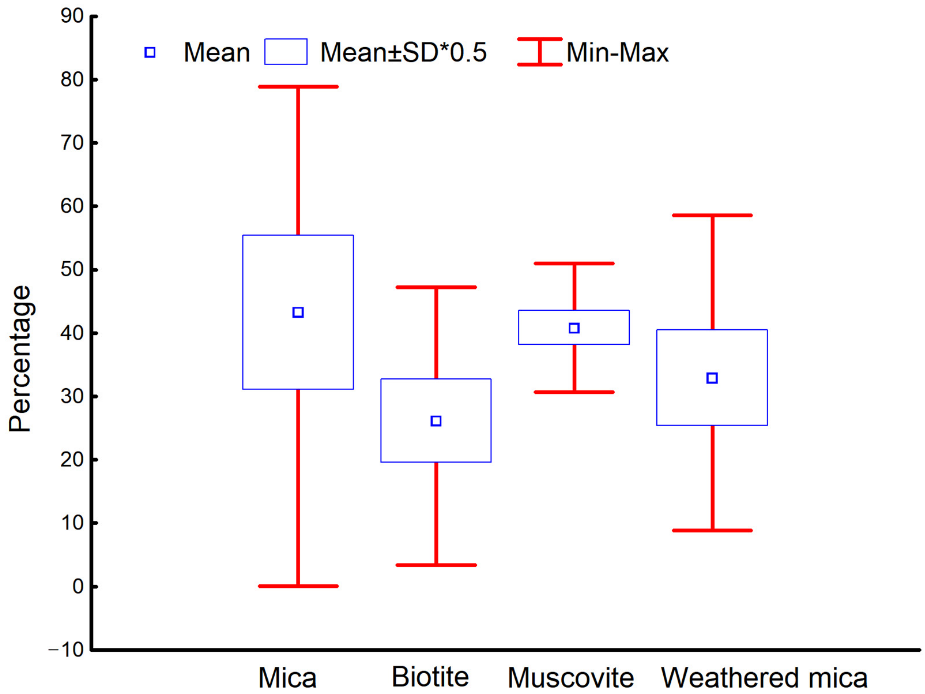

Figure 5. Mass percentage of mica and particle percentages of biotite, weathered mica and muscovite in the very fine sand fraction of Subei littoral plain area sediments (mass percentage of mica = 100 * total mica mass/total mineral mass. Particle percentage of biotite or weathered mica or muscovite = 100 * particle number of biotite or weathered mica or muscovite/total particle number of mica).

4. Discussion

4.1. Differences in Detrital Mica Contents in Sediments between the Yangtze River Estuary and Ancient Yellow River Estuary and the Causes of these Differences

Detrital minerals in sediments differ with the original rock, weathering degree, tectonic activity, climate change and other supergene environmental conditions [2,7], and micas are no exception. Their contents in large river sediments differ with watershed environments [7].

As shown in Figure 6, the contents and ratios of detrital mica in sediments between the Yangtze River Estuary and ancient Yellow River Estuary significantly differed. Specifically, the mass percentage of mica, particle percentage of weathered mica, particle percentage of muscovite, and particle percentage ratio of weathered mica to the sum of biotite and weathered mica in the very fine sand fraction of Yangtze River Estuary sediments were 2.47, 1.89, 1.15 and 2.06 times higher, respectively, than those in the very fine sand fraction of ancient Yellow River Estuary sediments. However, the particle percentage of biotite, particle percentage ratio of biotite to muscovite, and particle percentage ratio of the sum of biotite and weathered mica to muscovite in the very fine sand fraction of the ancient Yellow River Estuary sediments was 3.33, 4.05 and 1.28 times higher, respectively, than those in the very fine sand fraction of Yangtze River Estuary sediments. All of these results indicate that the mass percentage of mica and the particle percentage of weathered mica in the very fine sand fraction of the sediments in the Yangtze River Estuary were significantly higher than those in the very fine sand fraction of the sediments in the ancient Yellow River Estuary. The weathering degree of mica (the particle percentage ratio of weathered mica to the sum of biotite and weathered mica) was much higher than that in the ancient Yellow River Estuary. All of these results also suggested that the particle percentage of biotite and the particle percentage ratio of biotite to muscovite in the very fine sand fraction of the sediments in the ancient Yellow River Estuary were significantly higher than those in the very fine sand fraction of the sediments in the Yangtze River Estuary, although the weathering degree of mica was very low. Moreover, the particle percentage ratio of easily weathered mica (sum of biotite and weathered mica) to difficult-to-weather mica (muscovite) in the very fine sand fraction of the sediments in the ancient Yellow River Estuary was also higher than that in the very fine sand fraction of the sediments in the Yangtze River Estuary.

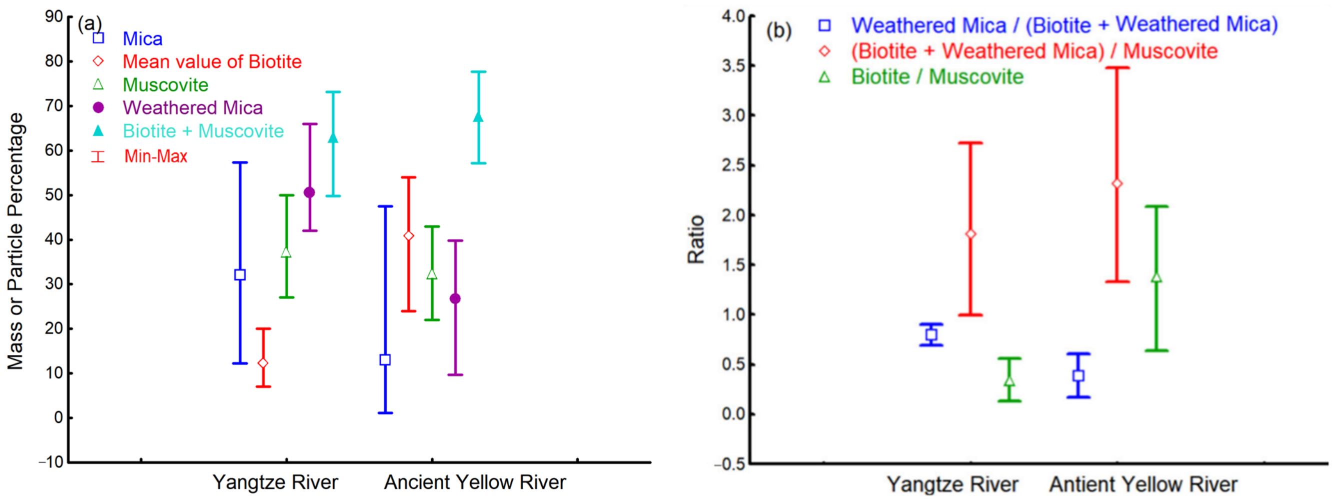

Figure 6. Comparison of the detrital mica contents (**a**) and ratios (**b**) in the very fine sand fraction of the sediments between the Yangtze River Estuary and ancient Yellow River Estuary. (**a**) shows the differences of mass percentage of mica (in bule) and particle percentages of biotite (in red), muscovite (in green), weathered mica (in purple) and sum of biotite and muscovite (in cyan). (**b**) shows the differences of particle percentage ratio of weathered mica to the sum of biotite and weathered mica (in blue), particle percentage ratio of the sum of biotite and weathered mica (in red), and particle percentage ratio of biotite to muscovite (in green).

Researchers have previously reported similar characteristics, such as high mica and muscovite contents in the very fine sand fraction of Yangtze River Estuary sediments, a high biotite content and high particle percentage ratio of biotite to muscovite in ancient Yellow River sediments. For example, Lv found that the content of schistose mica minerals in the 0.063–0.125 mm fraction of sediments in the Yangtze River Estuary was very high, with a maximum value of up to 60% [26]. This value was thought to represent a basic feature of the heavy mineral assemblages in the very fine-grained (0.063–0.125 mm) sediments of the Yangtze River Estuary [26]. Zhang and Meng also proposed that mica is one of the dominant minerals in Yangtze River Estuary sediments [33]. The highest mica content reached 32.4%, with a content of 17.1% in the silt fraction. Wang et al. noted that muscovite is one of the characteristic minerals of underwater delta sediments in the Yangtze River [54]. It was found that muscovite is widely distributed with moderate contents ranging from 5.7% to 2.5%, while biotite contents were lower, with the highest value of only 1.5% in the silty fraction. In addition, Lin et al. proposed that Yellow River materials were characterized by abundant mica minerals [25]. Biotite is one of the main minerals with high contents of up to 64.7% in underwater deltas. Muscovite is a secondary mineral and its content could reach approximately 5%. They also suggested that a high particle percentage ratio (value of 8.97) of biotite to muscovite could serve as a mineralogical indicator of Yellow River materials [25]. Wang et al. also found that the biotite content in Yellow River sediments (up to 23.36%) was much higher than that in Yangtze River sediments (very low) [55]. It was further suggested that mica in the 0.063–0.125 mm fraction of Yellow River Estuary sediments was the main dominant heavy mineral because its particle percentage reached 39.2% [32]. They also found that the muscovite content (17.6%) was higher than that of biotite (16.3%) and hydrobiotite (5.3%) [32].

In river basins, geological conditions, climate types and hydrodynamic conditions notably impact minerals in sediments [7,56], including detrital minerals. Thus, the causes of detrital mica differences in sediments between these two large river estuaries should be related to these factors (Figure 7). First, compared to the Yellow River drainage area, the exposed rocks in the Yangtze River drainage area are richer in mica. In the Yangtze River drainage area, granite, schist and gneiss are widely distributed in the middle-to-lower stream sections. This leads to a high content of detrital mica in Yangtze River sediments. However, in the Yellow River drainage area, loess widely covers the midstream area and is the main provenance of Yellow River detritus [35]. The mica content is approximately 18.4% in the >20 μm fraction of loess paleosol, with a maximum value lower than 26% [57]. This indicates that the mica content in the very fine sand fraction is not overly high in Yellow River sediments. Hence, the difference in geological conditions between provenance areas is an important reason why the mass content of mica in the very fine sand fraction of Yangtze River Estuary sediments is significantly higher than that in the very fine sand fraction of ancient Yellow River Estuary sediments. Second, compared to the Yellow River, the climatic conditions in the Yangtze River drainage area are more favorable for weathering. These climatic conditions include abundant precipitation and a high temperature in most areas of the Yangtze River drainage area, except for the upstream area. However, the region is dry and cold, with a lower annual precipitation and poor hydrothermal conditions in the Yellow River drainage area. Research has demonstrated that the chemical weathering rate (61.58 $t/km^2 \cdot a$) in the Yangtze River drainage area is significantly higher than that in the Yellow River drainage area (39.29 $t/km^2 \cdot a$) [58]. Strong chemical weathering in the Yangtze River drainage area inevitably leads to the release of a large number of mica minerals in igneous and metamorphic rocks, such as granite, into the river. Moreover, strong chemical weathering in the Yangtze River drainage area inevitably leads to the transformation of a large amount of biotite into weathered mica. Thus, the difference in weathering conditions is another important reason why the mass percentage of mica in the very fine sand fraction of the sediments in the Yangtze River Estuary is much higher than that in the very fine sand fraction of the sediments in the ancient Yellow River Estuary. This is also the main reason for the higher particle percentage of weathered mica in the very fine sand fraction of Yangtze River Estuary sediments and largely explains both the higher weathering degree of mica and the higher particle percentage of biotite. Third, in the Yangtze River Estuary, the flow velocity suddenly declines due to the low open flat trumpet-shaped terrain [59]. This terrain shape leads to the deposition of a large number of detritus [59]. Coupled with the controlling effect of seawater in the estuary and the disturbance of coastal currents, detrital mica easily affected by hydrodynamic forces also accumulates in this location. This is the third important reason for the higher mica content in the very fine sand fraction of the sediments in the Yangtze River Estuary. In contrast, mica originating from the Loess Plateau is resorted under the influence of stronger hydrodynamic forces in the estuary area of the ancient Yellow River. Moreover, due to the large differences in the particle size, density, shape, volume, and diameter-thickness ratio, the depositional velocity of mica is much lower than that of other minerals with the same particle size, such as quartz and feldspar. Thus, the particle size of mica settling in the very fine sand fraction is usually larger than that of other minerals, such as quartz and feldspar [28]. Research has demonstrated that the particle size difference between mica and other minerals in the same size fraction, such as quartz and feldspar, ranges from 1Φ to 1.5Φ [27]. This is also an important reason for the lower mass percentage of mica in the very fine sand fraction of ancient Yellow River Estuary sediments.

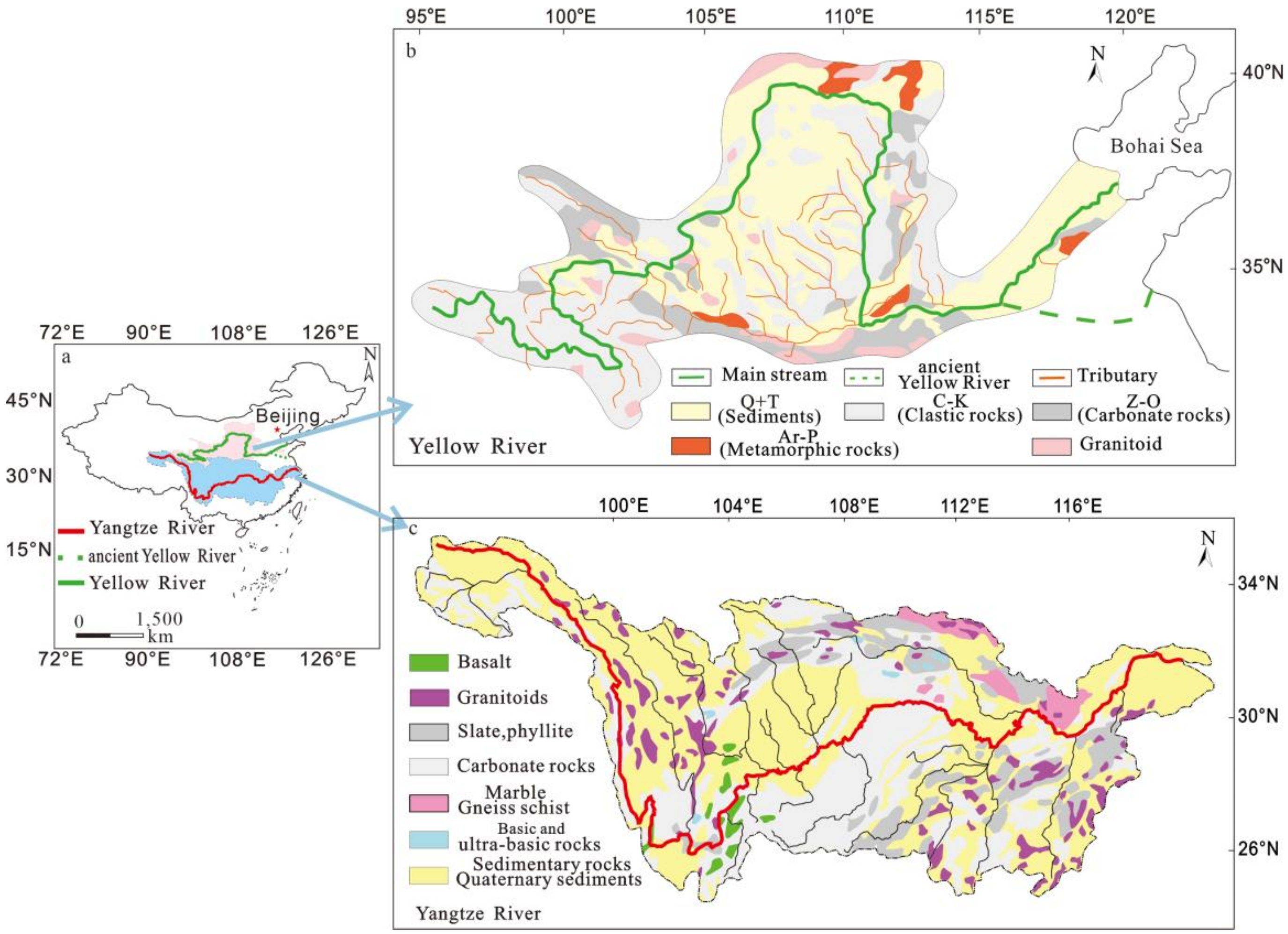

Figure 7. Geological map of the drainage basins in this study (modified based on Hongfei [60] and Wang [18]).

4.2. Specific Diagnostic Indices to Effectively Distinguish detritus between the Yangtze River Estuary and Ancient Yellow River Estuary

Micas in detrital sediments are divided into muscovite and biotite. Muscovite exhibits the most stable chemical properties and a high erosion resistance [61]. Biotite with unstable chemical properties is easily weathered [61]. Therefore, the differences and changes in mica indicators, such as the content and/or ratio, provide a certain significance to indicate provenance conditions, such as the watershed climate type and hydrothermal conditions.

Under the influence of the basic geology, climate and hydrodynamic forces in the source area, the detrital mica content and ratio in the very fine sand fraction of the sediments of the Yangtze River Estuary differ from those in the very fine sand fraction of the sediments in the ancient Yellow River Estuary. These differences make it possible to determine specific diagnostic indices for detritus to distinguish between these two large river estuaries.

As shown in Figure 8, four mica indices, including the particle percentage of biotite, particle percentage of weathered mica, particle percentage ratio of weathered mica to the sum of biotite and weathered mica and particle percentage ratio of biotite to muscovite, significantly differ between the Yangtze River Estuary and ancient Yellow River Estuary. Specifically, in the very fine sand fraction of Yangtze River Estuary sediments, these mica indices ranged from 6.67% to 19.85%, from 42.14% to 65.71%, from 0.69 to 0.90, and from 0.13 to 0.56, respectively. However, in the very fine sand fraction of ancient Yellow River Estuary sediments, these indices ranged from 24.41% to 53.93%, from 9.74% to 39.81%, from 0.17 to 0.60, and from 0.64 to 2.09, respectively. Thus, these specific diagnostic indices could be effectively used to distinguish detritus between these two river estuaries. These results are more detailed and specific than the existing research results. For instance, based on the characteristic of a high mica content in Yellow River sediments [24], Lin et al. proposed that the mica content could be used to distinguish the source and diffusion of marine sediments, identify coastline changes and determine the evolution of the paleogeographic environment [25]. They also suggested that a high particle percentage ratio of biotite to muscovite could be used as a mineralogical tracer parameter to distinguish the provenance of Yangtze River detritus [25]. In addition, Wang KS et al. proposed that mica minerals could be used as indicators of sediment transport and diffusion [32].

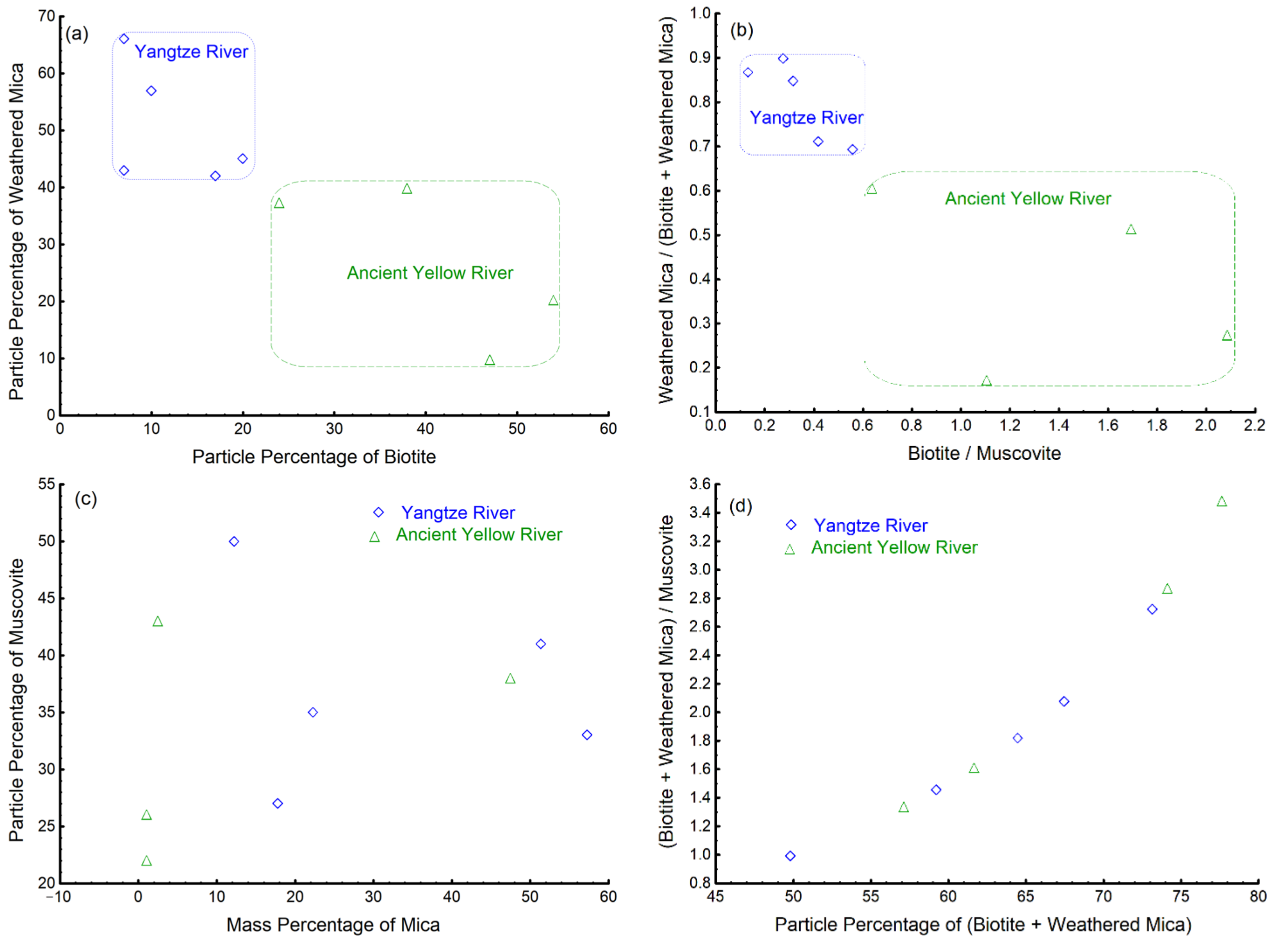

Figure 8. Index scatter diagrams of detrital mica in the very fine sand fraction of the sediments of the Yangtze River Estuary and ancient Yellow River Estuary; (**a**) particle percentage of biotite; (**b**) particle percentage ratio of weathered mica to the sum of biotite; (**c**) particle percentage of weathered mica; (**d**) weathered mica and particle percentage ratio of biotite to muscovite, significantly differ between the Yangtze River Estuary and ancient Yellow River Estuary.

4.3. Variation in the Mica-Specific Diagnostic Indices for the Very Fine Sand Fraction of Coastal Sediments in the Subei Littoral Plain Area and Provenance Significance

As previously mentioned, the four mica-specific diagnostic indices for effective detritus discrimination between the Yangtze River Estuary and ancient Yellow River Estuary include the particle percentage of biotite, particle percentage of weathered mica, particle percentage ratio of weathered mica to the sum of biotite and weathered mica, and particle percentage ratio of biotite to muscovite. Their numerical changes in the very fine sand fraction of sediments at different locations along the coast of the Subei littoral plain area are shown in Figure 9. These changes could effectively indicate the influence range of the Yangtze River and the ancient Yellow River on the coast of the Subei littoral plain area. These changes could be helpful to better explain the mixing area of these two sources at this location.

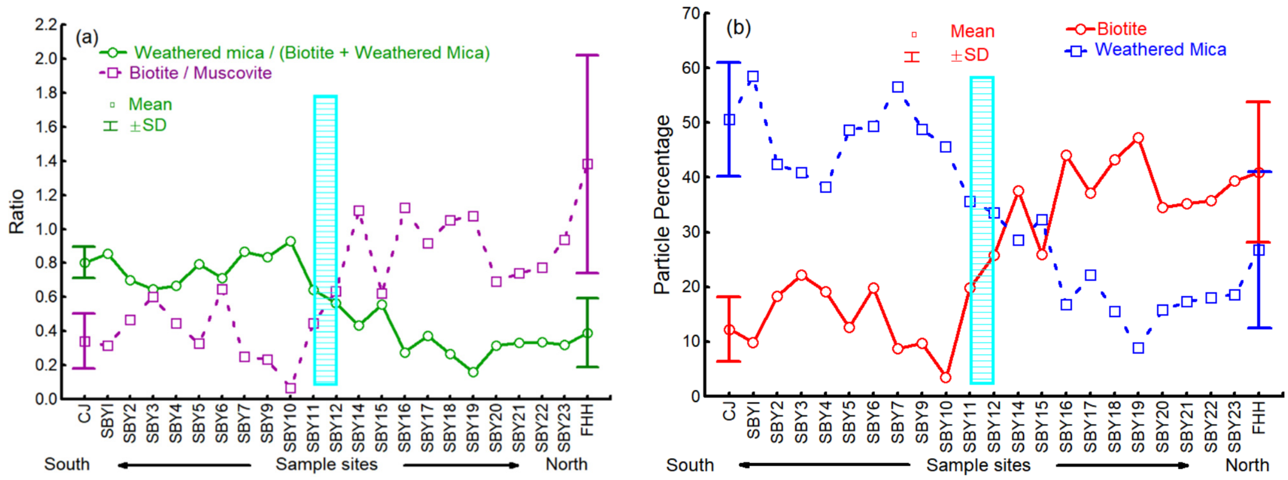

Figure 9. Variation in the mica-specific diagnostic indices in the very fine sand fraction of coastal sediments between the Yangtze River Estuary (CJ) and the ancient Yellow River Estuary (FHH) together with the Subei littoral plain area. (**a**) shows the variation of paticle percentage ratio of weathered mica to the sum of biotite and weathered mica (in green), and the variation of paticle percentage ratio of biotite to muscovite (in purple). (**b**) shows the variation of paticle percentage of biotite (in red) and weathered mica (in blue).

As shown in Figures 9 and 10, northward from the Yangtze River Estuary to Yangkou town in Rudong County (SBY11), the particle percentage of biotite and the particle percentage ratio of biotite to muscovite were low, while the particle percentage of weathered mica and the weathering degree of mica (the particle percentage ratio of weathered mica to the sum of biotite and weathered mica) were high. These values were close to those in the Yangtze River Estuary. This result indicates that detritus in the region along the coast northward from the Yangtze River Estuary to Yangkou town in Rudong County (SBY11) were mainly affected by Yangtze River detritus. This relationship is generally consistent with existing understandings. Li et al. suggested that the sediments southward from Rudong County to the Yangtze River Estuary could be dominated by Yangtze River detritus [43]. Changes in major element contents indicated that the northward diffusion range of Yangtze River sediments was smaller thanthe Yangtze River Estuary to the coast near Waya Port on the north side of Xiaoyangkou in Rudong County [42]. This area is close to the region of interest of this study. In addition, based on the characteristics of clay mineral assemblages, Yi et al. suggested that sediments from the coast southward from Rudong County to the Yangtze River Estuary were dominated by detritus inputs from the ancient Yangtze River [45].

Moreover, as shown in Figures 9 and 10, northward from Bencha town in Rudong County (SBY12) to the ancient Yellow River Estuary, the particle percentage of biotite and the particle percentage ratio of biotite to muscovite significantly increased, while the particle percentage of weathered mica and the weathering degree of mica (the particle percentage ratio of weathered mica to sum of biotite and weathered mica) significantly decreased. These values were close to those in the ancient Yellow River Estuary. This result indicates that detritus in the region along the coast northward from Bencha town in Rudong County (SBY12) to the ancient Yellow River Estuary were mainly affected by ancient Yellow River detritus. This relationship is also basically consistent with existing research results. For example, Zhao considered the area along the coast northward from Jianggang Port to the ancient Yellow River Estuary (close to the SBY13 sample site in Dongtai city in this study) to mainly be affected by the ancient Yellow River [41]. Based on the variation in the montmorillonite content, Zhang proposed that detritus along the coast northward from Rudong County to the ancient Yellow River Estuary originated from the ancient Yellow River [42]. By applying element geochemistry and heavy mineral methods, Yang et al. suggested that the land-forming process in the Subei littoral plain area was mainly controlled by the ancient Yellow River, with the southern boundary of influence near Xinhai Bore (near sample site SBY11 in this study) [43]. In addition, based on the characteristics of clay mineral assemblages, Yi et al. proposed that sediments from the coast northward from Rudong County to the ancient Yellow River Estuary were dominated by detritus inputs from the ancient Yellow River [45].

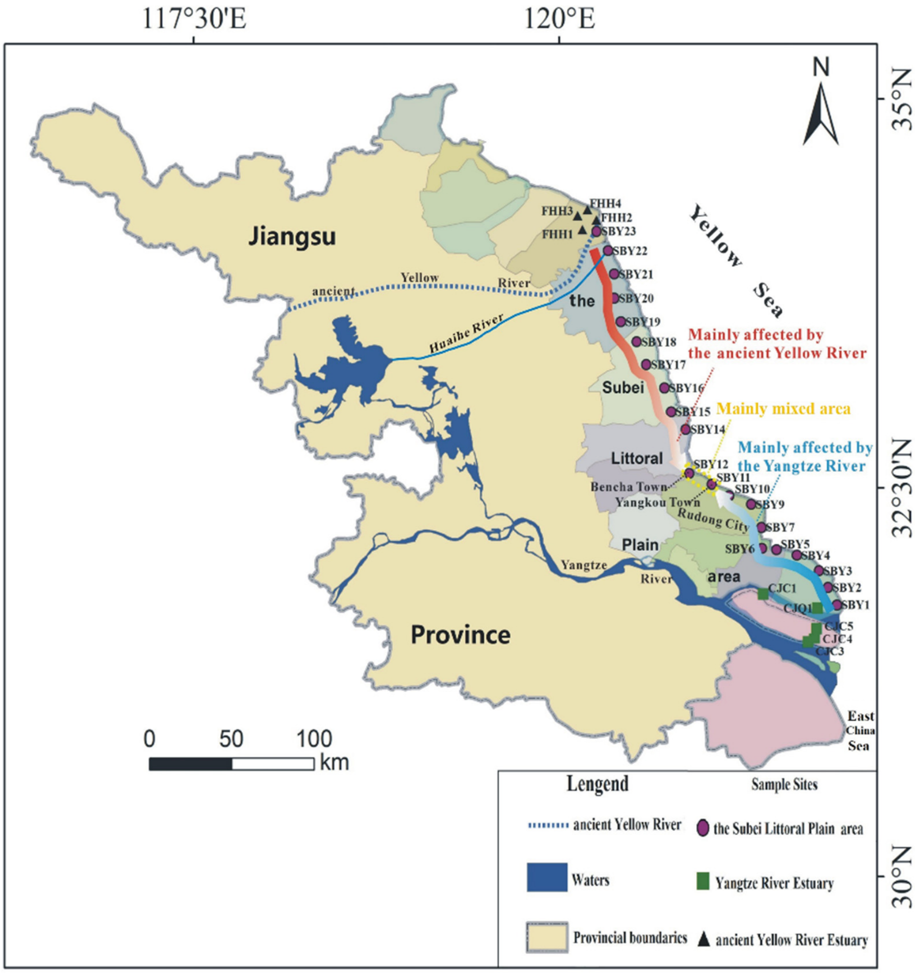

Figure 10. Ranges of the influence of the Yangtze River and the ancient Yellow River on detrital mica in the very fine sand sediments in the Subei littoral plain area.

In addition, as shown in Figures 9 and 10, compared to the four mica-specific diagnostic indices of the samples southward from SBY10 to the Yangtze River Estuary and northward from SBY14 to the ancient Yellow River Estuary, the index values at sample sites SBY11 and SBY12 were moderate. These results indicate that the main mixed area occurred between these two sites, i.e., SBY11 and SBY12. Detritus were mainly affected both by the Yangtze River and ancient Yellow River at this location. Yang et al. also proposed that between Dongtao Bore (near sample site SBY14) and Xinhai Bore (near sample site SBY11), the surface sediments at Sancang Bore (near sample site SBY12) were mainly mixed Yangtze River and ancient Yellow River sediments [43].

4.4. Quantitative Contributions of the Yangtze River and the Ancient Yellow River to Detrital Micas in the Subei Littoral Plain Area and Indicative Significance

The quantitative contributions of the Yangtze River and the ancient Yellow River to detrital mica in the very fine sand fraction of the sediments of the Subei littoral plain area are shown in Table 1. The coefficients of determination (R^2) are all more than 0.783 (Table 1). All of the variants explained are close to 100 (Table 1). Additionally, these quantitative contribution data are reliable (Figure 11). Thus, the mathematical model of provenance contribution based on mica-specific diagnostic indices for the very fine sand fraction of sediments is reliable. As indicated in Table 1, southward from sample sites SBY11 to SBY1, where SBY11 is located near Yangkou town in Rudong County and SBY1 is located close to the Yangtze River Estuary, the quantitative contributions of the Yangtze River (a_1) are all higher than 50%, while those of the ancient Yellow River (a_2) are lower than 50%. However, northward from SBY12 to SBY23, where SBY12 is located near Bencha town in Rudong County and SBY23 occurs near the ancient Yellow River Estuary, the quantitative contributions of the ancient Yellow River (a_2) are all higher than 50%, while those of the Yangtze River (a_1) are lower than 50%. In addition, it could be deduced from Table 1 that the mixed area of these two large rivers occurs between the SBY11 and SBY12. This deduction further confirms the correctness of the previous understanding obtained in this study.

Table 1. Quantitative provenance analysis results for the very fine sand fraction of the sediments in the Subei littoral plain area (a_1 is the contribution percentage of the Yangtze River, a_2 is the contribution percentage of the ancient Yellow River, $\varepsilon$is the contribution other unknown sources).

Samples	Regression Coefficient			Test Indices of the Regression Model			
	a_1	a_2	ε	Final Loss	R	R^2	Variance Explained
SBY1	1.00	0.00	1.39	61.6	0.987	0.973	97.3
SBY2	0.72	0.23	−0.03	0.01	1.00	1.00	100
SBY3	0.62	0.36	−0.05	0.01	1.00	1.00	100
SBY4	0.60	0.29	−0.04	0.03	1.00	1.00	100
SBY5	0.95	0.02	0.00	0.00	1.00	1.00	100
SBY6	0.90	0.10	1.53	14.7	0.995	0.991	99.1
SBY7	1.00	0.00	0.59	47.0	0.989	0.978	97.8
SBY9	0.97	0.00	−0.62	3.30	0.999	0.998	99.8
SBY10	0.92	0.00	−2.20	43.4	0.985	0.970	97.0
SBY11	0.53	0.33	−0.05	0.04	1.00	1.00	100
SBY12	0.39	0.51	−0.08	0.03	1.00	1.00	100
SBY14	0.10	0.89	−0.07	0.01	1.00	1.00	100
SBY15	0.36	0.53	−0.08	0.04	1.00	1.00	100
SBY16	0.00	0.99	−1.59	95.6	0.961	0.924	92.4
SBY17	0.00	0.90	−0.40	3.20	0.998	0.997	99.7
SBY18	0.00	0.96	−1.70	107.4	0.955	0.911	91.1
SBY19	0.00	0.99	−2.87	324.0	0.885	0.783	78.3
SBY20	0.00	0.80	−1.00	30.5	0.980	0.961	96.1
SBY21	0.00	0.82	−0.86	21.3	0.987	0.974	97.4
SBY22	0.00	0.84	−0.82	19.3	0.989	0.977	97.7
SBY23	0.00	0.91	−1.03	34.9	0.983	0.966	96.6

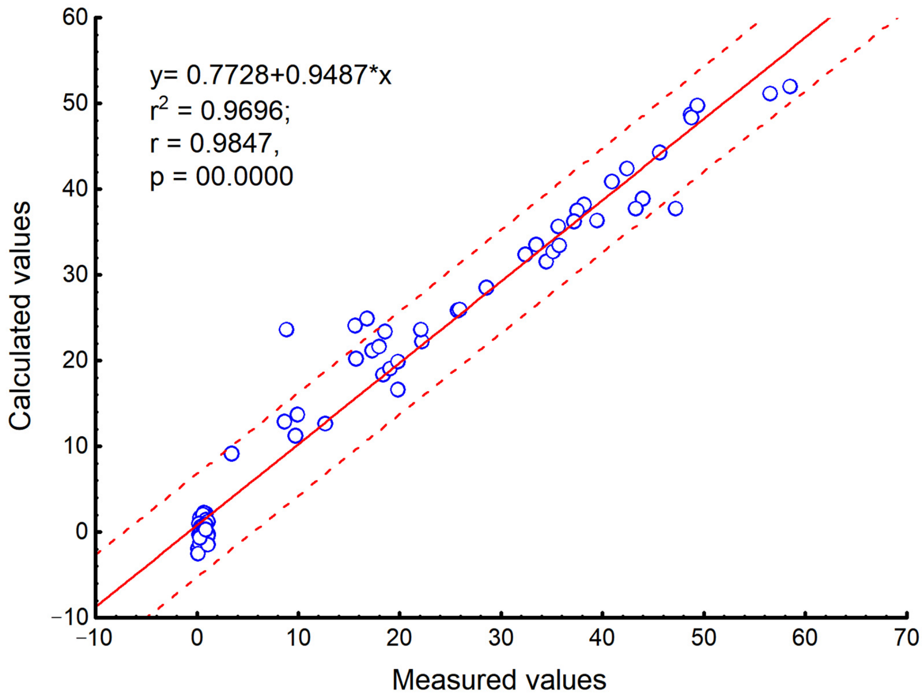

Figure 11. Scatter diagram for calculated values versus measured values of specific diagnostic indexes of detrital mica in the very fine sand fraction from sediments of the Subei littoral plain area (95% confidence).

5. Conclusions

Detrital mica contents were interestingly displayed and studied to identify two large rivers, namely the ancient Yellow River and the Yangtze River. Micas indices were selected and applied as provenance indicators to determine sediment contribution from the two rivers to the Subei coastal plain.

The contents and ratios of mica minerals in the very fine sand fraction of the sediments in the Yangtze River Estuary differed from those in the very fine sand fraction of the sediments in the ancient Yellow River Estuary. This difference could be attributed to a combination of different factors, such as basic geology, climate and estuarine hydrodynamics, in these two drainage area.

Four diagnostic indices were selected and used to effectively distinguish detritus in the Yangtze River Estuary and ancient Yellow River Estuary; these indices include the particle percentage of biotite, particle percentage of weathered mica, particle percentage ratio of weathered mica to the sum of biotite and weathered mica, and particle percentage ratio of biotite to muscovite. These indices ranged from 6.67% to 19.85%, 42.14% to 65.71%, 0.69 to 0.90, and 0.13 to 0.56, respectively, in the very fine fraction of Yangtze River Estuary sediments and 24.41% to 53.93%, 9.74% to 39.81%, 0.17 to 0.60, and 0.64 to 2.09, respectively, in ancient Yellow River Estuary sediments.

In the Subei littoral plain area, northward from the Yangtze River Estuary to SBY11 in Yangkou town, Rudong County, detrital micas were mainly affected by the Yangtze River. Moreover, in the Subei littoral plain area, southward from the ancient Yellow River Estuary to SBY12 in Bengcha town, Rudong County, detrital micas were mainly affected by the ancient Yellow River. In addition, the main mixing area of the Yangtze River and the ancient Yellow River occurred between these two sampling sites. The demarcation line between these areas could also be located in this region.

The above specific diagnostic indices of detrital mica could be employed for quantitative analysis of the provenances of detritus and their contributions.

Detrital mica in certain grain size fractions of sediments could be used for detritus identification, mixed area determination and provenance analysis.

Author Contributions: Conceptualization, Z.D. and L.Z.; Writing—Original manuscript Preparation, Z.D. and L.Z.; Writing—Review and Editing, L.Z. and B.J.; Ideas and experimental funds, L.Z. and B.J.; Data processing and Figures, Z.D. and L.Z.; Sampling and Experiments, L.Z. and B.J. All authors have read and agreed to the published version of the manuscript.

Funding: This study was supported by National Natural Science Foundation of China (41576057), Guangdong Basic and Applied Basic Research Foundation (2020A1515011077), Scientific Research Projects of Jiaying University (2020KJY05, 2019KJY05), Yantai Key Research and Development Plan (2019XDHZ103).

Institutional Review Board Statement: Not applicable.

Informed Consent Statement: Not applicable.

Data Availability Statement: It and all the data presented in this study are available on request from the corresponding author.

Acknowledgments: The authors would like to thank editors and all anonymous reviewers for their constructive suggestions and comments that helped to improve the quality of this paper.

Conflicts of Interest: The authors declare no conflict of interest.

Appendix A

Appendix A is the GPS locations of collected samples. It can be found online at https://data.mendeley.com/datasets/9f9y33rkm5/draft?a=c0bf25a2-f419-4bb9-acfb-b2564a9917df (accessed on 1 November 2022).

References

1. Wang, F.; Zhang, W.G.; Nian, X.M.; Andrew, P.R.; Zhao, X.; Shang, Y.; Ge, C.; Dong, Y. Magnetic evidence for Yellow River sediment in the late Holocene deposit of the Yangtze River Delta, China. *Mar. Geol.* **2020**, *427*, 106274. [CrossRef]
2. Zhang, W.G.; Xing, Y.; Yu, L.Z.; Feng, H.; Lu, M. Distinguishing sediments from the Yangtze and Yellow Rivers, China: A mineral magnetic approach. *Holocene* **2008**, *18*, 1139–1145. [CrossRef]
3. Zhang, W.G.; Ma, H.L.; Ye, L.P.; Dong, C.Y.; Yu, L.Z.; Huang, F. Magnetic and geochemical evidence of Yellow and Yangtze River influence on tidal flat deposits in northern Jiangsu Plain, China. *Mar. Geol.* **2012**, *319–322*, 47–56. [CrossRef]
4. Wang, K.S.; Shi, X.F.; Jiang, X.L. Sediment provenance and province of the southern Yellow Sea: Evidence from light mineral. *Chin. Sci. Bull.* **2003**, *48*, 30–36. [CrossRef]
5. Zou, L.; Dou, Y.G.; Hu, X.h.; Hu, B.Q.; Lin, X. Provenance analysis for surface sediments in different sepositional environments of the middle-south Okinawa Trough. *Mar. Geol. Quat. Geol.* **2021**, *41*, 115–124. (In Chinese with English Abstract)
6. Lu, J.; Li, A.C.; Zhang, J.; Huang, P. Yangtze River-derived sediments in the southwestern South Yellow Sea: Provenance discrimination and seasonal transport mechanisms. *J. Asian Earth. Sci.* **2019**, *176*, 353–367. [CrossRef]
7. Fan, D.J.; Yang, Z.S.; Mao, D.; Guo, Z.G. Clay minerals and geochemistry of the sediments from the Yangtze and Yellow rivers. *Mar. Geol. Quat. Geol.* **2001**, *4*, 7–12. (In Chinese with English Abstract)
8. Yang, Z.S. Mineralogical assemblages and chemical characteristics of clays from sediments of the Huanghe, Changjiang, Zhujiang Rivers and their relationship to the climate environment in their sediment source areas. *Oceanol. Limnetica Sin.* **1988**, *19*, 336–346. (In Chinese with English Abstract)
9. Zhang, Z.P.; Chu, Z.X. Modern variations in clay minerals in mud deposits of the Yellow and East China Seas and their geological significance. *Holocene* **2017**, *28*, 386–395. [CrossRef]
10. He, L.B.; Liu, Q.Y. Chemical characteristics of clay minerals in the sediments from the Yellow River and the Changjiang River. *Chin. Sci. Bull.* **1997**, *42*, 488–491. [CrossRef]
11. Zhao, J.S.; Zhou, J.; Chen, Q.; Zhen, K.G. Identification of Yangtze River and Yellow River Paleochannels in South Yellow Sea Shelf. *Adv. Mater. Res.* **2013**, *664*, 21–27. [CrossRef]
12. Yang, Z.S.; Fan, D.J.; Guo, Z.G.; Mao, D. Distribution of the carbonate clast size and the provenance analyses of the surface sediments in the northern East China Sea. *Acta Sedimentol. Sin.* **2002**, *20*, 1–6. (In Chinese with English Abstract)
13. Chen, J.; Chou, G.; Yang, J.D. Sr isotopic composition of carbonate in loess and identification of primary and secondary carbonate. *Prog. Nat. Sci.* **1997**, *6*, 731–734. (In Chinese with English Abstract)
14. Liu, D.S. *Loess and the Environment*; Science Press: Beijing, China, 1985; pp. 1–251. (In Chinese)
15. Yang, Z.S.; Wang, H.C.; Qiao, S.Q. Carbonate minerals in esturay sediments of the Changjiang and Huanghe: The content, morphology, and influential factors. *Oceanol. Limnetica Sin.* **2009**, *40*, 674–681. (In Chinese with English Abstract)
16. Zhang, J.Q.; Li, C.X.; Cong, Y.Z. Hydrodynamic environment and source of the old tidal sand body in the coastal plain of the northern Jiangsu. *Acta Oceanol. Sin.* **1998**, *20*, 82–90. (In Chinese with English Abstract)

17. Jin, B.F.; Wang, M.Y.; Yue, W. Comparative analysis of heavy mineral characteristics of sediments from the Huanghe River and the Changjiang River based on the multiple-window grain size strategy. *Cont. Shelf Res.* **2021**, *216*, 104326. [CrossRef]
18. Wang, Z.-B.; Li, R.-H.; Yang, S.-Y.; Bai, F.-L.; Mei, X.; Zhang, J.; Lu, K. Comparison of detrital mineral compositions between stream sediments of the Yangtze River (Changjiang) and the Yellow River (Huanghe) and their provenance implication. *China Geol.* **2019**, *2*, 169–178. [CrossRef]
19. An, Y.H.; Liu, J.; Zhang, J.Q.; Chen, B.; Chen, L.L.; Zhang, X.; Sheng, S. Comparative researches on the provenance indicators of Huaihe River, Yangtze River and Yellow River sediments. *Quat. Sci.* **2020**, *3*, 837–850. (In Chinese with English Abstract)
20. Yang, S.Y.; Jung, H.S.; Choi, M.S.; Li, C.X. The rare Earth element compositions of the Changjiang (Yangtze) and Huanghe (Yellow) River sediments. *Earth Planet. Sci. Lett.* **2002**, *201*, 407–419. [CrossRef]
21. Yang, S.Y.; Li, C.X.; Zhu, J.C.; Zhang, J.L. Provenance indicator of chemical fingerprint of magnetite in the Yangtze and Yellow river sediments. *Geochimica* **2000**, *5*, 480–484. (In Chinese with English Abstract)
22. Wang, Y.H.; Shen, H.T.; Zhang, W.G. A preliminary comparison of magnetic properties of sediments from the Changjiang and the Huanghe Estuaries. *Acta Sedimentol. Sin.* **2004**, *22*, 658–663. (In Chinese with English Abstract)
23. Lu, K.; Qin, Y.C.; Wang, Z.B.; Huang, L.; Li, G.X. Heavy mineral provinces of the surface sediments in central-southern East China Sea and implications for provenance. *Mar. Geol. Front.* **2019**, *35*, 20–26. (In Chinese with English Abstract)
24. Sun, B.Y. Detrital mineral assemblages in the Huanghe, Changjiang and Zhujiang Delta sediments. *Mar. Geol. Quat. Geol.* **1990**, *10*, 23–34. (In Chinese with English abstract)
25. Lin, X.T.; Li, W.R.; Shi, Z.B. Characteristics of mineralogy in the clastic sediments from the Yellow River provenance, China. *Mar. Geol. Quat. Geol.* **2003**, *23*, 17–21. (In Chinese with English Abstract)
26. Lv, Q.R. Mineral characteristics of fine-grain sediment and its sedimentary differentiation in Changjiang estuary. *Shanghai Geol.* **1992**, *43*, 18–25. (In Chinese with English Abstract)
27. Fan, S.M.; Jin, B.F.; Wang, X.; Yu, H.Y. Mica shape factor and its equivalent sedimentation in the sediment of the Yellow River Estuary. *Mar. Geol. Front.* **2021**, *5*, 31–38. (In Chinese with English Abstract)
28. Doyle, L.J.; Carder, K.; Steward, R.G. The Hydraulic Equivalence of Mica. *J. Sediment. Petrol.* **1983**, *53*, 643–648.
29. Sun, X.; Kuiper, K.F.; Tian, Y.; Li, C.; Gemignani, L.; Zhang, Z.; Wijbrans, J.R. Impact of hydraulic sorting and weathering on mica provenance studies: An example from the Yangtze River. *Chem. Geol.* **2019**, *532*, 119359. [CrossRef]
30. Gemignani, L.; Kuiper, K.F.; Wijbrans, J.R.; Sun, X.; Santato, A. Improving the precision of single grain mica 40Ar/39Ar-dating on smaller and younger muscovite grains: Application to provenance studies. *Chem. Geol.* **2019**, *511*, 100–111. [CrossRef]
31. Thierry, B.B.; Lebogang, M.; Chris, M.; Kelebogile, P.; Tebogo, K. Multistage gold mineralization events in the Archean Tati greenstone Belt, northeast Botswana: Constraints from integrative white mica Ar/Ar, garnet U-Pb and sulfides Pb/Pb geochronology. *Precambrian Res.* **2020**, *339*, 105623.
32. Wang, K.S.; Shi, X.F.; Cai, S.W.; Qiao, S.Q.; Jiang, X.L. Distribution and provenance of the surface sediments of the Yellow River Mouth and Laizhou Bay deduced from heavy minerals. *Mar. Geol. Quat. Geol.* **2010**, *30*, 1–8, (In Chinese with English Abstract). [CrossRef]
33. Zhang, F.Y.; Meng, Y. Heavy mineral distribution and magnetic characteristic of surface sediments in the north branch of the Changjiang River. *Mar. Geol. Quat. Geol.* **2011**, *31*, 31–41. (In Chinese with English Abstract) [CrossRef]
34. Hong, Q.Y.; Shi, M.D.; Cheng, H.T. *Changjiang Water Resources Commission. The History of Yangtze River*; Encyclopedia of China Publishing House: Beijing, China, 2007; pp. 25–77. (In Chinese)
35. Liu, J.P.; Milkman, J.D.; Gao, S.; Chen, P. Holocene development of the Yellow River's subaqueous delta North Yellow Sea. *Mar. Geol.* **2004**, *209*, 45–67. [CrossRef]
36. Xue, C.T.; Zhou, Y.Q.; Zhu, X.H. The Huanghe River course and delta from end of Late Pleistocene to the 7th century BC. *Acta Sedimentol. Sin.* **2004**, *26*, 48–61. (In Chinese with English Abstract)
37. Ren, M.E. *China's Three Deltas*; Higher Education Press: Beijing, China, 1994; pp. 56–73. (In Chinese)
38. Dai, Y.S. Basic characteristics of geological structure in the Yellow River Basin. *Yellow River* **1984**, *3*, 20–26. (In Chinese with English Abstract)
39. Ren, M.; Shi, Y. Sediment discharge of the Yellow River (China) and its effect on the sedimentation of the Bohai and the Yellow Sea. *Cont. Shelf Res.* **1986**, *6*, 785–810. [CrossRef]
40. Wang, Y.; Zhang, Z.K.; Zhu, D.K.; Yang, J.H.; Mao, L.J.; Li, S.H. River-sea interaction and the north Jiangsu plain formation. *Quat. Sci.* **2006**, *26*, 301–320. (In Chinese with English Abstract)
41. Zhao, Q.J. Influence of river on development of Jiangsu coast. *Mar. Sci.* **1992**, *3*, 53–55. (In Chinese with English Abstract)
42. Zhang, Y. A study of characteristics and sources of clay minerals of sediments in coastal areas of Jiangsu province. *Mar. Sci.* **1990**, *4*, 34–42. (In Chinese with English Abstract)
43. Yang, S.Y.; Li, C.X.; Zhang, J.Q. Palaeogeographic evolution of coastal plain and provenance study of postglacial sediments in north Jiangsu province. *J. Palaeogeogr.* **2000**, *2*, 68–75. (In Chinese with English Abstract)
44. Li, C.X.; Zhang, J.Q.; Fan, D.D.; Deng, B. Holocene regression and the tidal radial sand ridge system formation in the Jiangsu coastal zone, east China. *Mar. Geol.* **2001**, *1731*, 97–120, (In Chinese with English Abstract). [CrossRef]
45. Yi, S.Q.; Chen, B.B.; Wang, S.H. Numerical classification of clay minerals in beach soil of Jiangsu. *Acta Sedimentol. Sin.* **1998**, *25*, 349–355. (In Chinese with English Abstract)

46. Guo, Z.G.; Yang, Z.S.; Zhang, D.Q. Seasonal distribution of suspended matter in the northern East China Sea and barrier effect of current circulation on its transport. *Acta Oceanol Sin.* **2002**, *5*, 71–80. (In Chinese with English Abstract)
47. Liu, Z.L.; Hu, D.X.; Tang, X.H. Tidal current observation in the southern Yellow Sea in the summers of 2001 and 2003. *Chin. J. Oceanol. Limnol.* **2008**, *26*, 121–129. [CrossRef]
48. Chen, B.; Zhou, L.Y.; Liu, J.; Wang, K. The relationship between the suspended sediment movement and tidal current dynamic characteristic in Old Yellow Delta. *Mar. Sci.* **2011**, *5*, 73–81. (In Chinese with English Abstract)
49. Zhao, B.R.; Fang, G.H.; Cao, D.M. Characteristics of tidal residual currents and their relations with coastal current transports in the Bohai Sea, Yellow Sea and East China Sea. *Stud. Mar. Sin.* **1995**, *36*, 5–10.
50. Xia, C.S.; Qiao, F.L.; Yang, Y.Z.; Yuan, Y.L. Simulation of double cold cores of the 35° N section in the Yellow Sea with a wave-tide-circulation coupled model. *Chin. J. Oceanol. Limnol.* **2004**, *22*, 292–298.
51. Wu, H.; Gu, J.H.; Zhu, P. Winter Counter-Wind Transport in the Inner Southwestern Yellow Sea. *J. Geophys. Res. Ocean.* **2018**, *123*, 411–436. [CrossRef]
52. Ingersoll, R.V.; Bullard, T.F.; Ford, R.L.; Grimm, J.P.; Pickle, J.D.; Sares, S.W. The effect of grain size on detrital modes: A test of the Gazzi–Dickinson pointcounting method. *J. Sediment. Petrol.* **1984**, *54*, 103–116.
53. Fan, D.; Sun, X.; Yang, Z.; Guo, Z. A mathematical model on the quantitative provenance identification: Take the identification of the surface sediment sources from ECS as example. *Acta Sedimentol. Sin.* **2002**, *20*, 30–33. (In Chinese with English Abstract)
54. Wang, K.S.; Wang, G.Q.; Cai, S.W.; Dou, Y.G.; Shi, X.F.; Cheng, Z.B.; Jiang, X.L. Heavy mineral characteristics of surface sediments in the subaqueous Yangtze River Delta. *Mar. Geol. Quat. Geol.* **2007**, *1*, 7–12. (In Chinese with English Abstract)
55. Wang, L.C.; Chen, X.L.; Chu, T.Q. A contrast analysis on the loads character of the Changjiang River and the Yellow River. *Geogr. Res.* **1997**, *16*, 71–79. (In Chinese with English Abstract)
56. Weltje, G.J.; von Eynatten, H. Quantitative provenance analysis of sediments: Review and outlook. *Sediment. Geol.* **2004**, *171*, 1–11. [CrossRef]
57. Zheng, H.H.; Theng, B.K.G.; Whitton, J.S. Mineral composition of loess-paleosol in the Loess Plateau of China and its environment implication. *Geochimica* **1994**, *23*, 113–123. (In Chinese with English Abstract)
58. Li, J.Y.; Zhang, J. Chemical weathering processes and atmospheric CO_2 consumption of Huanghe River and ChangJiang River basins. *Sci. Geogr. Sin.* **2005**, *15*, 16–21. [CrossRef]
59. Chen, J.Y.; Yun, C.X.; Hu, H.G. The model of development of the Changjiang Estuary during the last 2000 years. In *Estuarine Comparisons*; Kennedy, V.S., Ed.; Academic Press: New York, NY, USA, 1982; pp. 655–666.
60. Hongfei, Z.; Yunhong, L.; Claudio, O.D.; Yue, M.; Jie, Z.; Hongming, H. Contribution of soil erosion to the evolution of the plateau-plain-delta system in the Yellow River basin over the past 10,000 years. *Palaeogeogr. Palaeoclimatol. Palaeoecol.* **2022**, *601*, 111133.
61. Pal, D.K.; Srivastava, P.; Durge, S.L.; Bhattacharyya, T. Role of weathering of fine-grained micas in potassium management of Indian soils. *Appl. Clay Sci.* **2001**, *20*, 39–52. [CrossRef]